

Empirical molecular dynamic study of SiC(0001) surface reconstructions and bonded interfaces

C. Koitzsch^{a)}

Technical University of Ilmenau, Weimarer Strasse 32, D-98693 Ilmenau, Germany

D. Conrad, K. Scheerschmidt^{b)} and U. Gösele

Max Planck Institute of Microstructure Physics, Weinberg 2, D-06120 Halle, Germany

(Received 27 June 2000; accepted for publication 3 October 2000)

Empirical molecular dynamics simulations based on the Tersoff potential are carried out for SiC(0001) surfaces and bonded interfaces. It is demonstrated that such a classical interatomic potential is able to correctly describe SiC-4H (0001) 3×3 and $\sqrt{3}\times\sqrt{3}R30^\circ$ surface reconstructions. The surprising accuracy of the empirical simulations compared to results of density functional methods as well as experiments is demonstrated not only by obtaining reasonable structural parameters, but also by the correct prediction of such intricate effects like buckling in the topmost carbon layer of the $\sqrt{3}\times\sqrt{3}$ surface and polymerization in the silicon wetting layer of the 3×3 reconstruction. Because of the established good applicability of the Tersoff potential the simulations are used to predict the formation of SiC interfaces to be generated by wafer bonding and so far experimentally unobserved. It is shown that the bond energy crucially depends on the local atomic structure at the interface. The resulting bond energies range from 0.56 up to 3.16 J/m² depending on the initially prepared reconstruction and alignment of the surfaces. © 2000 American Institute of Physics. [S0021-8979(00)09001-6]

I. INTRODUCTION

SiC received increasing attention during the last decade due to its interesting physical properties for electronic applications. The wide band gap, excellent thermal conductivity, and high temperature stability promise good applicability for high power devices and high temperature sensors. Nowadays different materials and their properties are compared by so called figures of merit, which summarize and emphasize certain physical properties in dependence on the desired application.¹ The high application potential of SiC for high power devices is represented by Baliga's figure of merit,² which exceeds the value for silicon by a factor of 106. High electron drift velocities and high breakdown fields are desirable for high frequency devices. The outstanding performance parameters of SiC in a variety of device structures have proven the maturity of SiC technology.³

The occurrence of more than 220 different polytypes is a very interesting crystallographic property and important for structures using SiC epitaxy. The most common forms are the hexagonal α -SiC, which is the wurtzite structure, and cubic β -SiC, which denotes the zinc-blende poly-type, and their various stacking combinations (4H-SiC, 6H-SiC, . . .). The band gap of the material varies for the different polytypes and ranges from 2.4 eV for the cubic 3C-SiC to 3.3 eV for the hexagonal 4H-SiC which has the shortest growable stacking sequence (see, e.g., Refs. 4 and 5). The combination

of perfectly lattice matched materials with different electronic gaps is attractive for homoepitaxial devices exhibiting behavior of a heterojunction. So far, multilayered devices based on SiC polytypism proved to be an extraordinary experimental challenge,⁶ due to difficulties in controlling the polytype evolution during growth. In a typical chemical vapor deposition or molecular beam epitaxy growth experiment steps of multiple bilayer height on the growth surface serve as a polytype seed. In contrast to the step morphology, the exposed surface itself does not deviate between polytypes, e.g., a 3C-SiC(111) and a 4H-SiC (0001) crystal. Coalescence on large islands apparently always leads to energetically favored 3C-SiC, while the step flow growth preserves the polytype of the SiC substrate. Starke *et al.*⁷ demonstrated that the different surface reactivity of reconstructions is responsible for the switch between the step flow growth and island growth, hence allowing polytype conservation or the growth of 3C-SiC, respectively.

The present article investigates a completely different approach for generating an electronically usable interface. Instead of growing different polytypes on top of each other, the interface generation by so called wafer bonding is simulated by means of empirical molecular dynamics (MD). Gösele *et al.*⁸ successfully demonstrated experimental silicon wafer bonding in UHV. This technique yields contamination free interfaces, which should be beneficial for the electronic characteristics.⁹ The silicon bonding experiments were accompanied by empirical MD, which simulated the interface generation on an atomic scale.^{10,11} Wafer bonding has become a widely recognized method to join similar and dissimilar materials and proved to be quite valuable for the silicon on insulator technology and for novel microelectro-

^{a)}Present address: University of Fribourg, Department of Physics, Perolles, CH-1700 Fribourg, Switzerland; electronic mail: Christian.Koitzsch@unifr.ch

^{b)}Author to whom correspondence should be addressed; electronic mail: schee@mpi-halle.de

mechanical systems and optical devices.¹² The effectiveness of the technology for pseudoheteroepitaxy using different SiC polytypes will be demonstrated by the presented MD simulations. The results of the simulation can serve as a guidance for experimentalists. The feasibility of SiC wafer bonding and the effects of different reconstructions are shown.

II. COMPUTATIONAL PROCEDURE

We used the empirical Tersoff potential^{13,14} for the MD simulations. In several applications of the Tersoff and extended potentials to include Si–C and other interactions,^{15–17} the ability of the empirical MD simulations are demonstrated to investigate surface reconstructions and chemisorption of hydrocarbons. After simulating differently reconstructed surfaces, i.e., the SiC(0001)-3×3 and $\sqrt{3} \times \sqrt{3}$ R30° reconstructions, we compared the structural parameters obtained by our simulations to existing experimental and theoretical models. The good agreement between simulations and experimental results in the case of surfaces encouraged us to extend the simulation to wafer bonded interfaces, specifically to the case of bonding of 3×3 and $\sqrt{3} \times \sqrt{3}$ R30° reconstructed surfaces. In both cases we investigated two basic arrangements, not yet successfully investigated experimentally. First we deal with a situation, in which the adhesion is only due to adatom–adatom bonds. In the second case the adhesion is due to the formation of an interlinked interface structure.

The molecular dynamics simulations were carried out using the NVT ensemble, i.e., constant number of atoms, constant volume and constant temperature. Supercells of 2.13 nm×1.85 nm×4.0 nm ($\sqrt{3} \times \sqrt{3}$ reconstructions) and 1.6 nm×1.85 nm×4.0 nm (3×3 reconstructions) were used. Periodic boundary conditions were applied in the plane of the surfaces. The free surfaces were relaxed at 0 K until the forces converged to less than 0.01 eV/Å. The simulations for interacting surfaces were carried out for room temperature until no bond rearrangement occurred anymore and then relaxed at 0 K, see, e.g., Ref. 10. The temperature stability was tested by simulating an annealing up to 1200 K.

III. RESULTS

A. Simulation of free surfaces

1. Simulation of the $\sqrt{3} \times \sqrt{3}$ R30° surface

Reconstructions with a $\sqrt{3} \times \sqrt{3}$ R30° periodicity are well known for a variety of adsorbed elements on different substrates, see, e.g., Refs. 18 and 19. Other possible structural elements besides single adatoms are vacancies or more complicated adclusters²⁰ in H3, T4, or S5 adsorption sites. For the SiC(0001) surface, these sites are located in the hexagon, above or below, respectively, the first carbon layer. The sites are schematically shown in Fig. 1(a). *Ab initio* calculations^{21–23} of the SiC $\sqrt{3} \times \sqrt{3}$ R30° surface have already indicated that silicon adatoms in T4 coordination are the energetically favorable arrangement. Simple symmetry considerations support this result. The T4 coordination yields a three-fold symmetry axis normal to the surface and centered at the adatom. The underlaying C atom is shifted down-

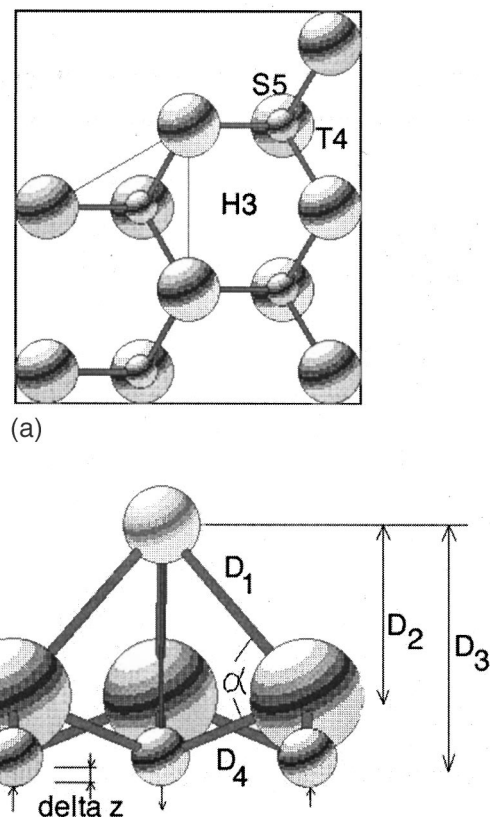


FIG. 1. (a) Top view of the 1×1 surface with T4, H3, and S5 adsorption sites. (b) Side view of the $\sqrt{3} \times \sqrt{3}$ R30° surface.

wards the surface, the surrounding C atoms are shifted upwards. The different shifts of the carbon atoms is the necessary prerequisite for a buckling relaxation of the underlying carbon layer, see Fig. 1(b). The theoretical model with Si adatoms in T4 sites was confirmed experimentally by Starke *et al.*⁷ via *I*–*V* low-energy electron diffraction (LEED).

At H3 sites the Si adatom is positioned in the center of SiC hexagons, which results in symmetric displacements. The S5 adsorption geometry allows a symmetric buckling, too, but does not correspond to scanning tunneling microscopy (STM) observations, which clearly showed protrusions and are therefore not compatible with subsurface sites.²⁴ However, photoemission experiments,²⁵ which had indicated a Si depleted top bilayer, may be interpreted as an indication for the S5 structure. As this case is not yet clarified, we did not use the S5 energy for comparisons.

Our molecular dynamics simulations based on the semi-empirical Tersoff potential support the silicon adatom T4 geometry. The single Si T4 adsorbate is energetically favored with respect to the H3 adsorption geometry by an amount of 0.38 eV per surface unit cell.

It is a reasonable approximation to relate this energy difference to the surface atoms because a relaxation deeper in the bulk was not observed and the bottom side atoms of the slab were fixed to the initial position. Krüger *et al.*²¹ calculated within density functional theory (DFT) an energy difference between H3 and T4 geometry of 0.6 eV per sur-

TABLE I. Structure parameters of the $\sqrt{3} \times \sqrt{3}$ R30° surface (distances D_1 – D_4 in angstroms, angles α and Δ in degrees, see Fig. 1).

Parameter	Local density approximation (LDA) calculation ^a	LEED Experiments ^b	This work
D_1	2.41–2.43	2.46	2.53
D_2	1.71–1.74	1.77	1.78
D_3	2.50–2.55	...	2.55
D_4	1.88	...	1.88
α	70–71.38	...	67.7
Δz	0.25–0.27	0.34	0.19

^aSee Refs. 21 and 23.

^bSee Ref. 35.

face unit cell, a value which supports the results of our simulations (see also Refs. 26–28). However, the analysis of the band structure by newer photoemission experiments²⁹ shows there are open questions to be clarified using enhanced simulations for the different models. The structural parameters of the different models are shown in Table I and Fig. 1.

2. Simulation of the 3×3 surface

The silicon excess on the surface revealed by Auger electron spectroscopy motivated Kaplan³⁰ to propose a model, consisting of two prominent protruding adatoms per unit cell and a stacking fault. The exact geometry of the SiC(0001)-3×3 reconstruction was thus first believed to be closely related to the standard Si(111)-7×7 dimer-adatom-stacking fault model.³¹ This model had to be modified after high quality STM works became available, which showed only one protrusion per unit cell, see Kulakov *et al.*³² The modified model consists of an incomplete silicon wetting layer with a silicon tetramer resting on, e.g., site 4 (cf. Figs. 2 and 3). This existence of 6 and 9 atomic rings on the surface surrounding vacancies was proposed. In a combined

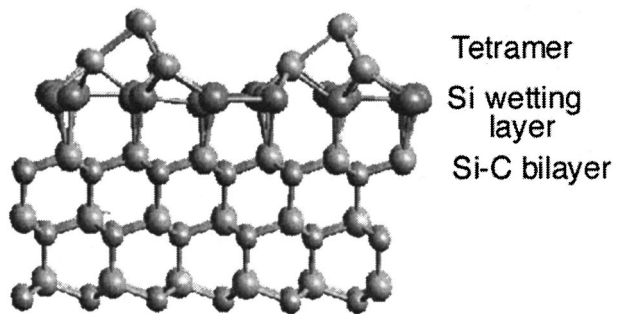


FIG. 3. Side view of the 3×3 reconstruction.

effort of dynamical LEED analysis guided by DFT,³³ the Kulakov model was further refined by modifying the structure of the first silicon wetting layer. Essentially, it was proposed that the adlayer does not exhibit vacancies. Without a rearrangement this would imply that some silicon atoms like atom 11 in Fig. 2 exhibit three dangling bonds, which is highly unlikely. Instead, relaxation is believed to take place and leading to the formation of five and seven membered Si rings. This polymerization-like rearrangement passivates the surface, since the number of dangling bonds is reduced by the corresponding formation of sp^2 hybrids. The present empirical MD simulation again supports the current surface model. The structural parameters of simulations are compared to the current model in Table II. The formation of the polymer-like ring structure strongly depends on the starting conditions of our simulation. By manually moving the atoms in the expected position it was shown that in terms of the Tersoff potential the polymerized surface is a minimum energy configuration. However, a self-ordering towards such a configuration from an ideal truncated bulk was not observed in our simulations.

B. Simulation of wafer bonded interfaces

After testing the Tersoff potential for *a priori* well-known surfaces and proving its applicability even for slight relaxation effects such as buckling and polymerization, simulations of the structure of bonded SiC wafers were performed. In this case, presently no experimental observations are available.

Wafer bonded interfaces are simulated with the original parameter set of the Tersoff potential.^{14,34} The simulation of interfaces should be even more appropriate for the used pa-

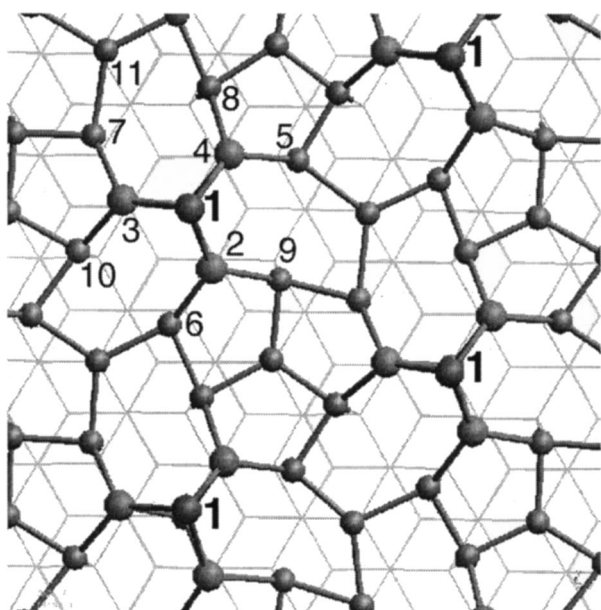
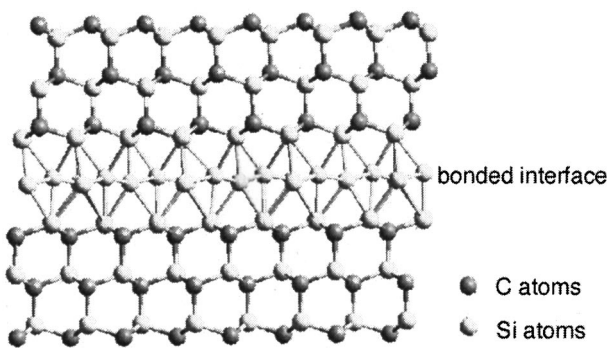


FIG. 2. Top view of the 3×3 reconstruction (filled circles denote Si adsorbate sites, clearly visible are five and seven membered atomic rings; bulk lattice and bilayer faintly sketched).

TABLE II. Structure parameter of the 3×3 surface (bl=bond length in angstroms, ba=bond angle in degrees, see Figs. 2 and 3).

Parameter	LEED/LDA ^a	This work
bl 1–2,3,4	2.47	2.56
bl 2,3,4–6,7,5	2.35	2.42
bl 2,3,4–9,10,8	2.31	2.40
bl 5,6,7–11	2.39	2.46
ba 2,3,4–1–3,4,2	88.80	84.55
ba 6,7,5–2,3,4–9,10,8	97.60	93.80
ba 5,6,7–11–6,7,5	120.00	120.00

^aSee Ref. 33.

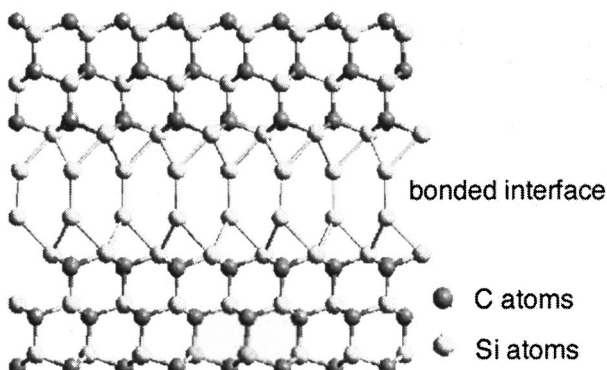
FIG. 4. $\text{SiC}\sqrt{3}\times\sqrt{3}\text{R}30^\circ$ surfaces: bonding in chainsaw arrangement.

rameters, since they were initially obtained by fitting bulk properties, e.g., the bulk bond length and elastic moduli, a situation which is closer to an interface than a surface. In contrast to the simulation of free surfaces, no atoms were held fixed at their starting position, allowing intimate contact of the two wafers facing each other. Two types of starting surfaces prior to bonding were considered: one type consisted of a surface reconstructed with a 3×3 structure and the other type with a $\sqrt{3}\times\sqrt{3}\text{R}30^\circ$ periodicity. A total of four different arrangements were investigated: free surfaces of each type were aligned such that either the topmost adatoms were juxtaposing (peak-to-peak, or equivalently adatom \parallel adatom) or the corresponding top atoms were arranged in a chainsaw-like structure. All the starting configurations were arranged in such a way that at least some atoms of the two opposing surfaces had a distance just below the cutoff radius of the Tersoff potential for initiating the bonding process.

Rotated arrangements were not investigated since the necessary unit cell for periodic boundary conditions is much larger for small misorientations. Since $\text{SiC}(0001)1\times 1$ surfaces are commonly assigned to disordered surface structures caused by impurities, no effort was undertaken to model this rather undefined situation.

1. $\sqrt{3}\times\sqrt{3}\text{R}30^\circ$ arrangement

The simulation showed that the relaxation of both initial configurations of Figs. 4 and 5 leads to stable configurations. The stability was also tested at temperatures up to 1000°C .

FIG. 5. $\text{SiC}\sqrt{3}\times\sqrt{3}\text{R}30^\circ$ surfaces: bonding in peak-to-peak arrangement.TABLE III. Packing density (in percent) and bond energy (in J/m^2).

Interfaces	Packing density	Bond energy
$\sqrt{3}\times\sqrt{3}\text{R}30^\circ$ adatom \parallel adatom	13.96	1.64
Interlinked $\sqrt{3}\times\sqrt{3}\text{R}30^\circ$	19.9	3.16
3×3 adatom \parallel adatom	28.58	0.56
Interlinked 3×3	47.53	2.9

and no disintegration was observed. This indicates that both simulations lead to a local minimum in the potential energy surface.

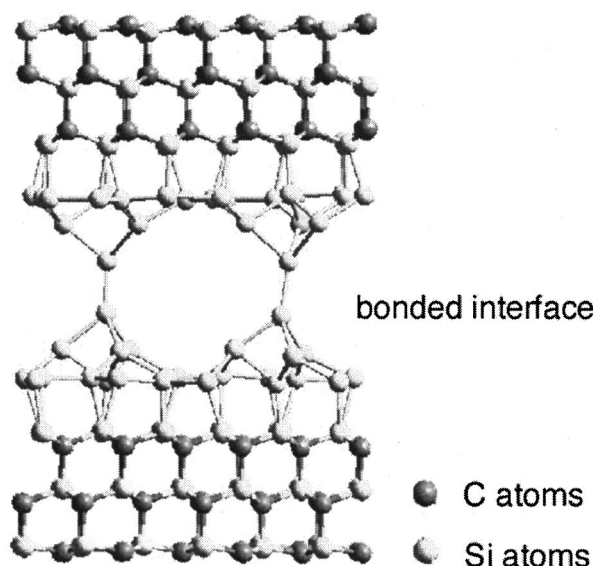
For the interlinked chainsaw structure, the formation of lateral interactions in the xy plane could be observed. This interaction induces the formation of atomic rows diagonally to the initial reconstruction, i.e., in $[1\bar{1}0]$ or $[2\bar{1}10]$ direction depending on the initial conditions. An equilibrium row length could not be detected but the number of silicon atoms in one row ranges from dimers up to five atoms. In our simulation, an alignment of adatoms and empty T4 sites was not energetically favored.

Comparison of the peak-to-peak and the chainsaw arrangement shows that an interlinking yields a much higher packing density of silicon atoms of the interface [Here we used *packing density* = (*number of silicon interface atoms*) / ($z_{\text{Si-C bilayer } 1} \cdot z_{\text{Si-C bilayer } 2} \cdot A_{\text{supercell}}$) with z being the number of atoms and A the area per supercell.]. The number of silicon atoms per interface volume of course is not necessarily correlated to the local atomic coordination, which determines the bond energy. However, in the case of comparing wafer bonded interfaces with $\sqrt{3}\times\sqrt{3}\text{R}30^\circ$ initial reconstruction, packing density and bond energy seem to be correlated, see Table III. The bond energy was determined after a relaxation at elevated temperatures up to 600°C . The more open structure and missing linkage for the peak-to-peak configuration easily accounts for the reduction in bond energy during annealing, attraction is only due to a single Si–Si bond across the interface per surface unit cell.

2. Simulation of wafer bonded interfaces with initial 3×3 reconstruction

The 3×3 peak-to-peak arrangement is quite similar to the $\sqrt{3}\times\sqrt{3}\text{R}30^\circ$ one. The initial configuration consists of two opposing 3×3 reconstructions with the top silicon adatoms separated by 2.77 \AA in z direction and no offset in the xy plane. Again the adatoms, which are initially only three-fold coordinated and exhibit therefore a dangling bond state are solely responsible for the attraction of the two crystals. Since the 3×3 reconstructed surface exhibits large corrugations, the interface is comprised of large holes (see Fig. 6) with a low packing density of the interface. The missing interaction between other components of the surface leads to a preservation of the structural parameters of the initial reconstruction.

If the starting configuration is modified by slightly translating the surface unit cells of the crystals facing each other such that an ad-tetramer is opposite to the silicon wetting layer instead of an ad-tetramer, a completely different behavior occurs. After narrowing the gap between the two crystals

FIG. 6. SiC 3×3 surfaces: bonding in peak-to-peak arrangement.

to the interaction radius of the Tersoff potential, bond breaking and rearrangement starts. The tetramer arrangement on top of the silicon wetting layer splits up and the broken bond of the adatom leads to bonding of the opposing tetramer or even the opposing wetting layer. Three-, four-, and five-fold coordinated interface silicon atoms were observed. In our simulations, no periodicity could be detected, even after extensively annealing the structure. The bond energy of the resulting dense amorphous structure is 2.9 J/m^2 compared to 0.56 J/m^2 for the peak-to-peak arrangement. Both values were determined after relaxing the sample at 300 K for more than 10 ps.

IV. CONCLUSIONS

It has been shown that the Tersoff potential is well suited to describe the SiC 3×3 and $\sqrt{3}\times\sqrt{3}\text{R}30^\circ$ surface reconstructions. A comparison to recent TB and DFT results^{21,26–28} shows that even the bond lengths and energy differences of the reconstructions are correctly accounted for. Especially the prediction of buckling in the carbon layer for the $\sqrt{3}\times\sqrt{3}\text{R}30^\circ$ surface and of polymerization of the first silicon wetting layer for the 3×3 surface look quite promising. The structural results are in good agreement with experimental LEED studies. The good quality of the Tersoff potential might be helpful in modeling other experimentally observed reconstructions in the silicon–carbon system.

Simulation of wafer bonded interfaces revealed the detailed dependence of the bond energy on the local atomic environment. Different starting configurations yielded bond energies between 0.5 and 3.2 J/m^2 . These values are in the range of experimentally obtained adhesion energies of silicon wafer bonding.¹² The low packing density and low bond energy of the 3×3 peak-to-peak arrangement suggest that the occurrence of this arrangement is unlikely in experiments. The amorphous interlayer resulting in the MD simulations for the second investigated 3×3 configuration shows that

this configuration may not be useful for electronic applications using SiC bonded interfaces, in which electric current has to cross the interface and thus also the most likely highly resistive amorphous interlayer.

The calculated bond energies of 1.64 and 3.16 J/m^2 , respectively, for the $\sqrt{3}\times\sqrt{3}\text{R}30^\circ$ reconstructed surface promise more success in bonding experiments due to the higher reactivity of this type of surface due to the higher density of dangling bonds per area. In addition, there is a good chance that the experimental verification may be accomplished since, in contrast to the 3×3 surface, the $\sqrt{3}\times\sqrt{3}\text{R}30^\circ$ reconstruction is the less Si rich one so that the formation of epitaxial Si clusters are more likely to be avoided during surface preparation. Therefore, we predict that the formation of contamination free SiC wafer-bonded interfaces can be achieved by preparing $\sqrt{3}\times\sqrt{3}\text{R}30^\circ$ reconstructed surfaces in an ultrahigh vacuum environment.

ACKNOWLEDGMENTS

C.K. appreciates the hospitality during his stay at MPI and would like to thank Professor R. J. Nemanich from North Carolina State University for his advice on the experimental side of bonding SiC surfaces.

- ¹L. M. Porter and R. F. Davis, Mater. Sci. Eng. B **34**, 83 (1995).
- ²B. J. Baliga, *Power Semiconductor Devices* (PWS, Boston, 1996).
- ³C. H. Carter *et al.*, Mater. Sci. Eng. B **61–62**, 1 (1999).
- ⁴P. Käckell and F. Bechstedt, Appl. Surf. Sci. **104–105**, 490 (1996).
- ⁵K. Karch, P. Pavone, W. Windl, and D. Strauch, Phys. Rev. B **502**, 17054 (1994).
- ⁶A. Fissel, U. Kaiser, J. Kräusslich, K. Pfennighaus, B. Schröter, J. Schulz, and W. Richter, Mater. Sci. Eng. B **61–62**, 139 (1999).
- ⁷U. Starke, J. Schardt, J. Bernhardt, M. Franke, and K. Heinz, Phys. Rev. B **82**, 2107 (1999).
- ⁸U. Gösele, H. Stenzel, T. Martini, J. Steinkirchner, D. Conrad, and K. Scheerschmidt, Appl. Phys. Lett. **67**, 3614 (1995).
- ⁹R. Stengl, K. Y. Ahn, T. Mii, W.-S. Yang, and U. Gösele, Jpn. J. Appl. Phys., Part 1 **28**, 2405 (1989).
- ¹⁰D. Conrad, K. Scheerschmidt, and U. Gösele, Appl. Phys. A: Mater. Sci. Process. **62**, 7 (1996).
- ¹¹K. Scheerschmidt, D. Conrad, A. Belov, and D. Timpel, Mater. Sci. Semicond. Process. **3**, 129 (2000).
- ¹²A. Plössl and G. Kräuter, Mater. Sci. Eng. R. **25**, 1 (1999).
- ¹³J. Tersoff, Phys. Rev. B **39**, 5566 (1989).
- ¹⁴J. Tersoff, Phys. Rev. B **38**, 9902 (1989).
- ¹⁵D. W. Brenner, Phys. Rev. B **42**, 9458 (1990).
- ¹⁶A. J. Dyson and P. V. Smith, Surf. Sci. **396**, 24 (1998).
- ¹⁷D. R. Alfonso and S.E. Ulloa, Appl. Phys. Lett. **74**, 55 (1999).
- ¹⁸V. Cimalla, Th. Stauden, G. Ecke, F. Schermann, G. Eichhorn, J. Pezoldt, S. Sloboshanin, and J. A. Schaefer, Appl. Phys. Lett. **73**, 3542 (1998).
- ¹⁹J. Quinn and F. Jona, Surf. Sci. Lett. **249**, L307 (1991).
- ²⁰J. Quinn, F. Jona, and P. M. Marcus, Phys. Rev. B **46**, 7288 (1992).
- ²¹P. Krüger, M. Sabisch, and J. Pollmann, Phys. Rev. B **55**, 10561 (1997).
- ²²P. Käckell, J. Furthmüller, and F. Bechstedt, Diamond Relat. Mater. **6**, 1346 (1997).
- ²³J. E. Northrup and J. Neugebauer, Phys. Rev. B **52**, 17001 (1995).
- ²⁴U. Starke, M. Franke, J. Bernhardt, J. Schardt, K. Reuter, and K. Heinz, Mater. Sci. Forum **264–268**, 321 (1998).
- ²⁵L. I. Johansson, F. Owman, and P. Martensson, Phys. Rev. B **53**, 13793 (1996).
- ²⁶L. Pizzagalli, A. Catellani, G. Galli, F. Gygi, and A. Baratoff, Phys. Rev. B **60**, R5129 (1999).
- ²⁷R. Gutierrez, M. Haugk, J. Elsner, G. Jungnickel, M. Elstner, A. Siech, T. Frauenheim, and D. Porezag, Phys. Rev. B **60**, 1771 (1999).

- ²⁸M. Rohlffing and J. Pollmann, Phys. Rev. Lett. **84**, 135 (2000).
²⁹L. S. O. Johansson, L. Duda, M. Laurenzis, M. Kriefenwirth, and B. Reihl, Surf. Sci. **445**, 109 (2000).
³⁰R. Kaplan, Surf. Sci. **215**, 111 (1989).
³¹Y. Ma, S. Lordi, and J. A. Eades, Surf. Sci. **313**, 317 (1994).
³²M. A. Kulakov, G. Henn, and B. Bullemer, Surf. Sci. **346**, 49 (1996).
³³J. Schardt *et al.*, Phys. Rev. Lett. **80**, 758 (1998).
³⁴D. Conrad, Ph.D. thesis, Martin Luther University, Halle, Germany, 1996.
³⁵J. Bernhardt, J. Schardt, U. Starke, and K. Heinz, Appl. Phys. Lett. **74**, 1084 (1999).